

The Discovery of Ledipasvir (GS-5885): The Potent Once-Daily Oral HCV NS5A Inhibitor in the Single-Tablet Regimen Harvoni[®]



John O. Link

Contents

1	Introduction	58
2	Discovery Work Leading to Ledipasvir	62
3	Ledipasvir (1, LDV, GS-5885)	67
4	Translation of Ledipasvir's Preclinical Potency and PK Properties in Phase I Clinical Trials	71
5	LDV/SOF Approval and Real-World Data	76
6	Conclusion	78
	References	78

Abstract The advent of direct-acting antiviral agents (DAAs) has revolutionized the treatment and cure of chronic hepatitis C virus (HCV) infection. Herein is described the discovery of ledipasvir (LDV), an orally available HCV nonstructural protein 5A inhibitor with picomolar antiviral potency and a long pharmacokinetic half-life. The combination of LDV with the nonstructural protein 5B inhibitor sofosbuvir (SOF) is Harvoni[®] and represents the first approved single-tablet regimen for the treatment of HCV infection. This safe simple and efficacious regimen affords clinical trial cure rates over 95% and comparable effectiveness in real-world studies and has treatment durations as short as 8 weeks. The approval of Harvoni[®] heralded a new era for the treatment of HCV infection.

Keywords Direct-acting antiviral, GS-5885, Harvoni[®], HCV, LDV/SOF, Ledipasvir, NS5A inhibitor, NS5B nucleotide inhibitor, Single-tablet regimen

J. O. Link (✉)
Medicinal Chemistry, Gilead Sciences, Foster City, CA, USA
e-mail: John.link@gilead.com

1 Introduction

Prior to the direct-acting antiviral (DAA) era, the standard of care for HCV-infected individuals included toxic, poorly tolerated regimens based on ribavirin (RBV) and some form of interferon (IFN) and resulted in low SVR (cure) rates. Among the six major HCV genotypes, IFN-based regimens unfortunately resulted in the lowest cure rates for genotype 1 (GT1) patients, the most prevalent genotype worldwide (Fig. 1, US Veterans Administration) [1].

The complexity, poor response rates, and toxicity of IFN-based regimens are underrepresented by the SVR rates reported from clinical studies and the common description that these regimens engender “flu-like” symptoms. Real-world results present a more accurate picture of the patient’s experience. The real-world efficacy of interferon regimens (cure rates outside of clinical trials) is vastly lower than even the ~30–50% SVR results reported from controlled clinical trials. Real-world efficacy late in the IFN era produced SVR as low as 3% in a report of 13,000 patients in 25 real-world studies across the United States (Fig. 2) [2]. This exceedingly low cure rate is a consequence of many factors, including a large number of exclusion criteria and significant toxicity and complexity of the regimen that precipitates patient discontinuation, hesitance to start therapy, and viral breakthrough and relapse [2].

Based on the poor results observed from the IFN-based standard of care, many patients deferred therapy in hope of newer treatment approaches while their liver

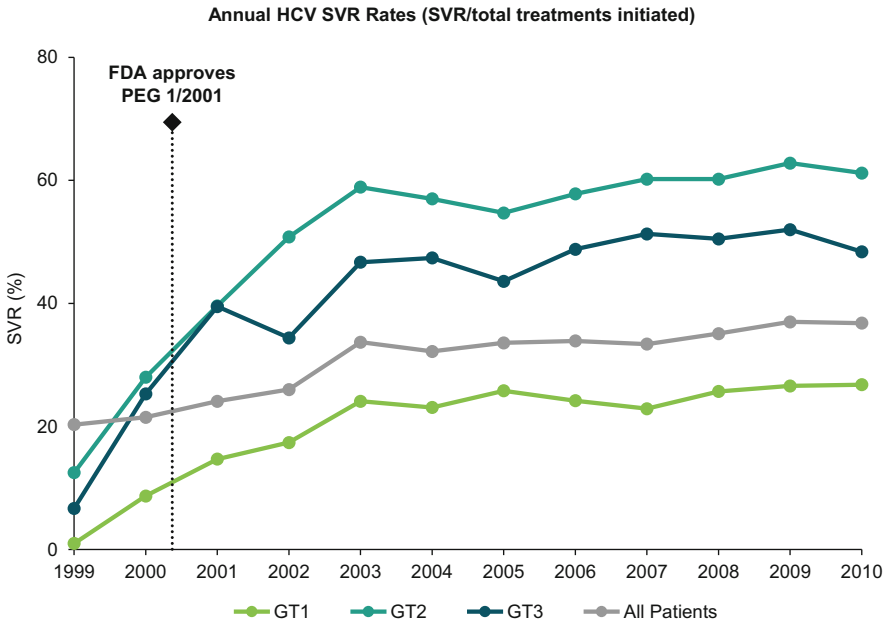


Fig. 1 SVR rates are the lowest for GT1 patients with IFN-based regimens

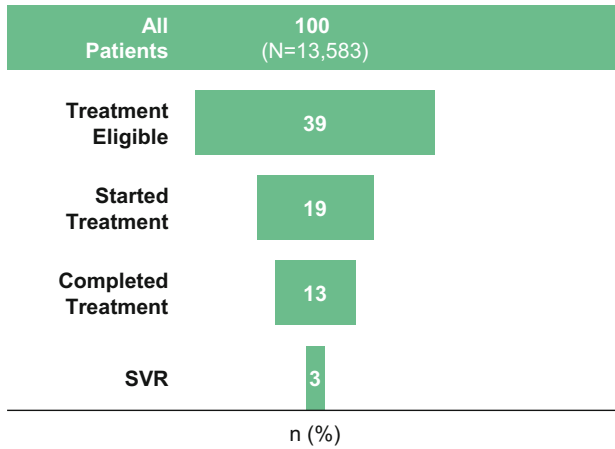


Fig. 2 Real-world IFN regimen results. 25 studies (2002–2012) show much lower SVR rates than those reported from clinical trials

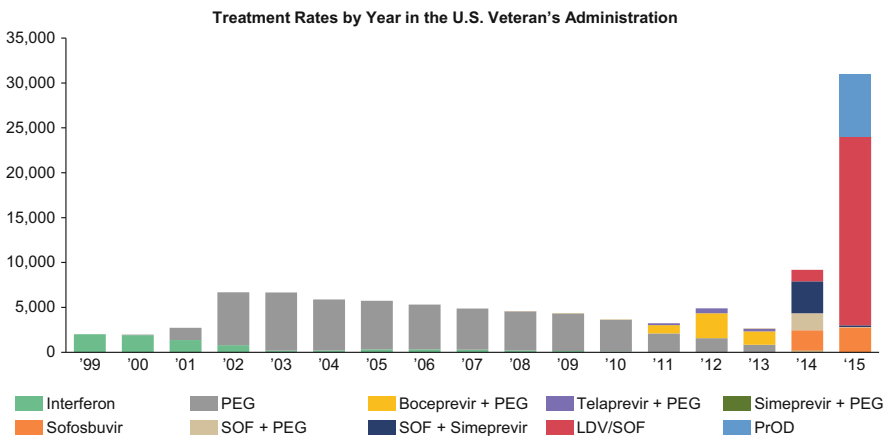


Fig. 3 Treatment rates increase sharply with the introduction of DAAs, particularly the STR LDV/SOF. *Interferon* beta-interferon, *PEG* pegylated interferon, *PrOD* paritaprevir, ritonavir, ombitasvir, dasabuvir

disease progressed to advanced stages of fibrosis or cirrhosis (Fig. 3) [1]. In 2013 as a consequence of the aging HCV-infected patient population progressing to liver cirrhosis, fibrosis, and hepatocellular carcinoma, the Center for Disease Control disclosed that deaths arising from HCV infection in the United States had surpassed those of all other notifiable infections combined in the United States (including human immunodeficiency virus [HIV], tuberculosis, and influenza) [3]. There was a critical need for improved therapies.

The advent of DAA therapies marked a revolution in the treatment and cure of HCV infection. The rapid uptake of DAA therapy underscores the high unmet need

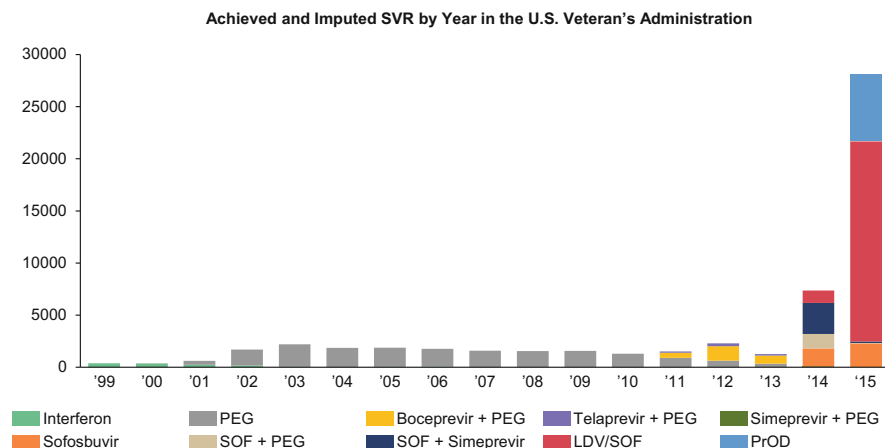


Fig. 4 The low SVR rates from the IFN era (compare to Fig. 3) are transformed during the DAA era. *Interferon* beta-interferon, *PEG* pegylated interferon, *PrOD* paritaprevir, ritonavir, ombitasvir, dasabuvir

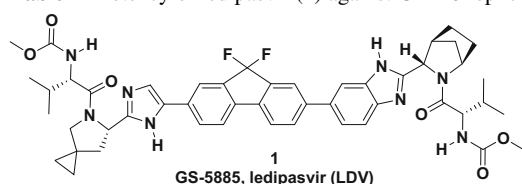
that existed in HCV therapy, with telaprevir (2011) and then sofosbuvir (2013)^{1,2} [4] and finally the combination drug ledipasvir/sofosbuvir (2014)³ [5] each becoming the largest drug launches in history [6–9]. The benefit to patients in this progression of DAAs can be seen in Figs. 3 and 4 which show treatment rates and cure rates in the US Veterans Administration progressing from the IFN era to the approval and uptake of LDV/SOF [1].

With the high level of unmet need for HCV patients in the IFN era as a backdrop, we pursued multiple viral and host targets for the treatment of HCV infection. At the time of initiating our efforts to discover an HCV nonstructural protein 5a (NS5A) inhibitor, we had over 20 HCV research programs ongoing, and several compounds undergoing, or selected to enter clinical trials. The more advanced agents, GS-9190 (NS5B non-nucleotide polymerase inhibitor), GS-9256, and GS-9451 (NS3/4a protease inhibitors), were directed at inhibiting GT1 HCV [10–12]. As a result of both the lower response rates to IFN therapy and high prevalence (with GT1 infection estimated to be as high as 60% of HCV-infected individuals worldwide [13]), there was a dominant unmet need for improved treatment of GT1 HCV infection. Based on this epidemiological and therapeutic landscape, we initiated our NS5A inhibitor program with primary potency assays directed toward GT1 HCV antiviral activity. This chapter details the discovery and early development of the potent HCV NS5A inhibitor ledipasvir (**1**, GS-5885, Table 1) and its clinical combination with sofosbuvir [14]. The discovery program toward the pan-genotypic NS5A inhibitor

¹https://www.accessdata.fda.gov/drugsatfda_docs/label/2015/204671s0021bl.pdf. Accessed 4 Dec 2018.

²Volume I, HCV: The Journey from Discovery to a Cure.

³https://www.accessdata.fda.gov/drugsatfda_docs/label/2015/205834s0011bl.pdf. Accessed 10 June 2018.

Table 1 Potency of ledipasvir (**1**) against GT1–6 replicons and subtypes

	HCV GT EC ₅₀ (pM) ^a									
	1a ^b	1b ^c	2a ^d	2aJ6 ^e	2b ^f	3a ^g	4a ^h	5a ⁱ	6a ^j	6e ^k
LDV	31	4	21,000	249,000	530,000	168,000	390	150	1,100	264,000

^aCheng G et al. *J. Hepatol.* 2013;58(suppl):S484. http://www.natap.org/2013/EASL/EASL_34.htm. Last accessed June 10, 2018

^bGT1a (strain H77)

^cGT1b Con-1

^dGT2a JFH-1

^eGT2a J6

^fGT2b MD2b-1 NS5A

^gGT3a S52 transiently transfected subgenomic HCV replicon

^hGT4a ED43

ⁱGT5a SA13 NS5A (9-184) transient chimeric replicons based on GT1b Rluc backbone

^jGT6a HK6 stable subgenomic HCV replicon

^kGT6e D88 NS5A (9-184) transient chimeric replicons based on GT1b Rluc backbone. In these replicons a–c, f, and g are stable subgenomic replicon cells; d and e are NS5A transient chimeric replicons based on GT2a JFH-1 Rluc backbone

velpatasvir initiated immediately following our ledipasvir discovery work. The discovery of our pan-genotypic NS5A inhibitor velpatasvir (VEL, GS-5816) is described in Volume II, HCV: The Journey from Discovery to a Cure and the following references: [15–17]. The discovery of our pan-genotypic NS3/4a protease inhibitor voxilaprevir (VOX, GS-9857) and its combination with SOF and VEL as Vosevi[®] is described in Volume I, HCV: The Journey from Discovery to a Cure and the following references: [18]. (https://www.accessdata.fda.gov/drugsatfda_docs/label/2017/209195s0001bl.pdf. Accessed 10 June 2018).

We targeted our NS5A inhibitor to possess properties appropriate for incorporation with one or more other HCV antiviral agents in a single-tablet regimen (STR). Single-tablet regimens have proven beneficial for patient compliance and efficacy in the chronic treatment of HIV infection [19, 20]. We saw a similar utility for an STR in the treatment of HCV infection. Thus the attributes of our NS5A inhibitor required sufficient potency and metabolic stability to achieve a low dose, a long pharmacokinetic half-life compatible with once-daily dosing, and a drug interaction profile suitable for combination with other HCV antivirals of complementary mechanism. The research program focused on these principles to guide the optimization of potency and pharmacokinetic (PK) parameters in the discovery of LDV. LDV is combined with SOF as Harvoni[®], and LDV was the first US Food and Drug Administration (FDA) approved NS5A inhibitor (October 10, 2014). Harvoni[®] was approved for the treatment and cure of GT1 HCV-infected individuals in as short as

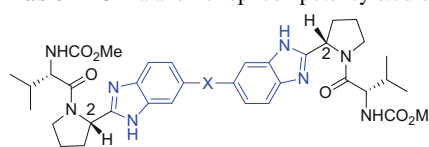
8 weeks of therapy and was the first approved HCV STR. Based on the potent antiviral activity of LDV against GT4, GT5, and GT6 HCV (Table 1), and the concomitant high SVR rates for LDV/SOF in GT4–6 patients, Harvoni[®] was additionally approved for treatment of GT4–6 patients (https://www.accessdata.fda.gov/drugsatfda_docs/label/2015/205834s001lbl.pdf. Accessed 10 June 2018) [5].

2 Discovery Work Leading to Ledipasvir

We focused on discovering an NS5A inhibitor that could be utilized in a single-tablet regimen in combination with other HCV agents. Further, we sought high antiviral potency and a long PK half-life to reduce the potential for emergence of viral breakthrough or resistance during treatment [14]. A large number of diverse cores were designed and synthesized in the discovery of LDV [21]. In early studies we investigated symmetric core inhibitors (where the core is the portion of the inhibitor structure that spans from between the C2 positions of each [modified] pyrrolidine – as colored in blue in Table 2). Potency proved challenging to attain against the genotype 1a subtype (GT1a) replicon but was more readily attained against the genotype 1b subtype (GT1b). Thus potency discussions herein most typically refer to GT1a potency, with GT1b potency provided in tables for reference. Throughout this manuscript, potency values represent effective concentration to reduce replication by 50% (EC_{50}) in cell lines with engineered replicons.

Table 2 outlines potency optimization for structural variation within the core between two benzimidazoles. With directly linked benzimidazoles, compound **2** does not achieve an EC_{50} against GT1a at the top concentration of 44,000 pM. Alkyne **3** is 138 pM against GT1b, but again is not active against GT1a. Bis-alkyne **4** improves GT1a potency to 11,000 pM. Incorporation of ring systems further improves potency. Thiophene- and phenyl-based cores improve potency from 1,700 to 500 pM, respectively. Biphenyl (**6**) loses activity relative to phenyl (**5**), while fused-ring systems provide highly potent inhibitors with naphthyl (**7**) and benzodithiophene (**8**) achieving 110 pM and 200 pM GT1a inhibition, respectively.

The inhibitors in Table 3 represent a shift in our thinking and provide the initiation of a fruitful path that we investigated throughout our NS5A inhibitor program. The inhibitors in Table 3 have unsymmetric cores, where one end of the core is a benzimidazole and the other end an imidazole. The use of unsymmetric cores has implications that will be discussed further (vide infra). Our unsymmetric approach afforded intriguing structural variation and properties to our inhibitors and afforded striking divergences from the results for the bis-benzimidazole cores in Table 2. In the imidazole/benzimidazole series, interestingly the phenyl-based core inhibitor **9** does not achieve 50% inhibition at the highest assay concentration and is >88-fold weaker in activity than in the bis-benzimidazole example (**5**). Most striking is that replacement of phenyl (**9**) by naphthyl (**10**) in this series affords an increase in potency by 620-fold. Despite significant divergence in potency for the phenyl inhibitors between these series, in both series the naphthyl-based core provides the

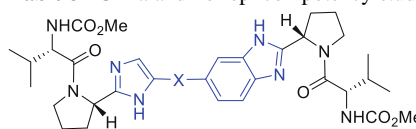
Table 2 GT1a and 1b replicon potency studies in symmetric core (core portion in blue) inhibitors


Compound	X	EC ₅₀ (pM)	
		GT1a ^a	GT1b ^b
2	Bond	>44,000 ^c	35,400
3		>44,000 ^c	138
4		11,000	26
4		1,700	10
5		500	9
6		3,700	44
7		110	4
8		200	16

^aGT1a (strain H77)^bGT1b Con-1; in this manuscript, these are the replicon strains for GT1a and GT1b^cA value of “>44,000 pM” means that the EC₅₀ was not achieved at this top well concentration

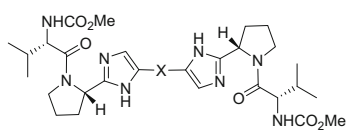
most potent inhibitor against GT1a observed within each table of inhibitors (compounds **7** and **10**). It is also notable the unsymmetric core inhibitor **10** at 71 pM in GT1a is more potent than the symmetric inhibitor **7**. Phenyl-alkynyl inhibitors **11** and **12** reveal another important facet of these unsymmetric cores. With the core possessing unsymmetric ends (imidazole/benzimidazole), and with the presence of unsymmetric central “-X-” groups, there is a matched and mismatched combination within the core. The core with the phenyl attached to the imidazole (inhibitor **12**, 380 pM versus GT1a) affords 6.6-fold more potency than the core with the alkynyl attachment to the imidazole. Finally, replacement of the alkyne with an aryl group provides potent biaryl inhibitors. The biphenyl inhibitor **14** is 22-fold more potent at 170 pM in GT1a than the corresponding inhibitor in the bis-benzimidazole series.

Fused-ring cores in Tables 2 and 3 afforded three out of the top four most potent inhibitors (**7**, **8**, and **10**, ranging from 70 to 110 pM versus GT1a). The biphenyl-based inhibitor **14** was the only non-fused-ring core that attained high potency (170 pM) comparable to the fused-ring cores. Importantly inhibitor **14** was stable at the lower measured limit of our routine human liver microsomes (HLM) stability

Table 3 GT1a and 1b replicon potency studies in unsymmetric core (portion in blue) inhibitors


Compound	X	EC ₅₀ (pM)	
		GT1a	GT1b
9		>44,000 ^a	300
10		71	7
11		2,500	16
12		380	11
13		200	3
14		170	7

^aA value of “>44,000 pM” means that the EC₅₀ was not achieved at this top well concentration



X:

				
15	16	17	18	
GT1a EC ₅₀ (pM)	94	300	1200	7000
GT1b EC ₅₀ (pM)	13	18	14	14

Fig. 5 Fused tricyclic core-based inhibitor potency

assay (predicted clearance <0.16 L/h/kg), whereas the naphthyl inhibitor **10** demonstrated less metabolic stability in microsomes. The favorable potency and metabolic stability of the biaryl inhibitor **14**, along with our observation that fused-ring systems provide high potency, prompted us to combine these concepts through constraint of the biphenyl to afford a tricyclic fused-ring inhibitor series.

These tricycle-based core inhibitors (Fig. 5) were synthesized in a symmetric bis-imidazole core series allowing for an easier synthetic path than the unsymmetric series and a more rapid assessment of the tricyclic systems. Fluorene **15** showed good potency but was unstable even to air oxidation. The oxidation product, fluorenone **16**, was less potent, and dimethyl substitution to block the system from oxidation lost over 13-fold in potency. The exo-dimethylmethylene was synthesized

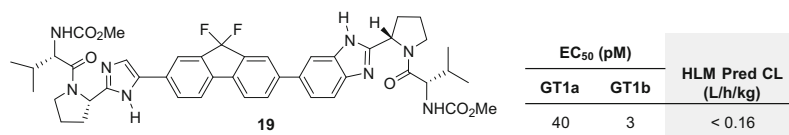


Fig. 6 Difluorofluorene **19** affords improved potency and oxidative stability and has good PK half-lives

Table 4 Rat and dog pharmacokinetics^a

Compound	Spec	CL (L/h/kg)	V _{ss} (L/kg)	t _{1/2} (h)	MRT ^a (h)	%F
14	Rat	1.04 ± 0.17	1.76 ± 0.17	1.57 ± 0.19	1.71 ± 0.16	11.5 ± 8.7
	Dog	0.78 ± 0.29	2.31 ± 0.37	2.30 ± 0.28	3.00 ± 0.27	n.d. ^c
19	Rat	0.42 ± 0.04	0.93 ± 0.04	1.83 ± 0.22	2.21 ± 0.21	36.7 ± 3.2
	Dog	0.53 ± 0.04	1.96 ± 0.03	2.63 ± 0.18	3.69 ± 0.29	n.d. ^c
21	Rat	0.70 ± 0.02	0.98 ± 0.08	1.49 ± 0.02	1.40 ± 0.07	35.2 ± 10
	Dog	0.05 ± 0.007	0.31 ± 0.007	5.29 ± 0.60	6.60 ± 1.10	n.d. ^c
22	Rat	0.75 ± 0.04	1.81 ± 0.26	2.07 ± 0.19	2.42 ± 0.22	26.3 ± 9.0
	Dog	0.40 ± 0.26	2.03 ± 0.92	4.01 ± 0.82	5.47 ± 1.01	n.d. ^c

All parameters except %F are from intravenous dosing

^aMean residence time

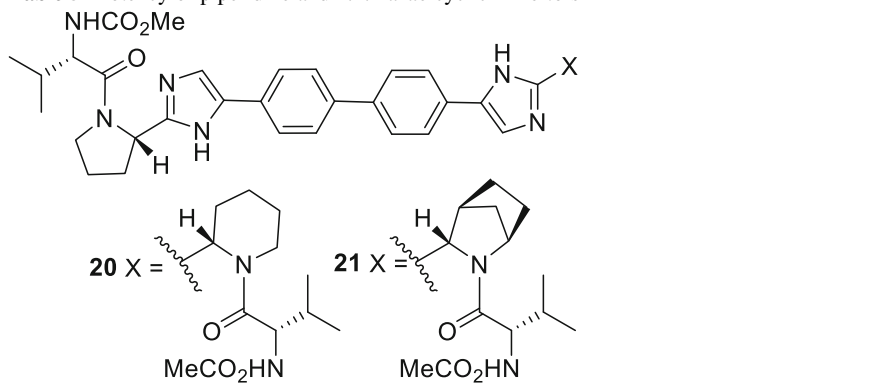
^bn.d. not determined

to avoid the out-of-plane bulk of **17** and the dipole of **16** but suffered a 78-fold potency loss relative to fluorene **15**. (It is intriguing that GT1b activity tightly ranges from 13 to 18 pM over this series.)

We sought to synthesize the difluorofluorene to block the fluorene methylene oxidation with a relatively small group – installation of two fluorines on the methylene proved challenging, and we incorporated them in the high value unsymmetric series (Fig. 6). The unsymmetric difluorofluorene-based core afforded inhibitor **19** with the highest potency in this series at 40 pM in GT1a and 3 pM in GT1b and was stable under the conditions of the HLM assay.

Unsymmetric biphenyl (**14**) and difluorofluorene (**19**) inhibitors were progressed into rat and dog PK (Table 4). Both inhibitors displayed good pharmacokinetic properties with moderate steady-state volumes of distribution (V_{ss}) higher than total body water. Difluorofluorene **19** had superior and low clearance in both rat and dog, longer half-lives, and greater bioavailability in rat than biphenyl inhibitor **14** (36.7% versus 11.5%). Thus difluorofluorene **19** showed improvements in potency and pharmacokinetic properties over biphenyl **14**.

Next a number of terminal heterocycle modifications were undertaken, again in a symmetric series for simplification of chemical synthesis. The azabicyclo[2.2.1] inhibitor **21** was more potent than piperidine **20** (Table 5). Although not as potent as the more advanced inhibitors such as **19**, azabicyclic inhibitor **21** displayed

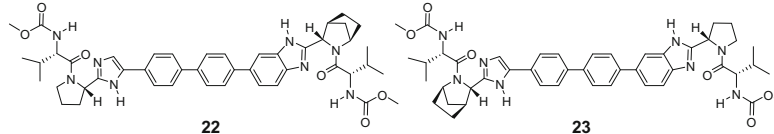
Table 5 Potency of piperidine and 2.2.1 azabicyclic inhibitors


	20	21
GT1a EC ₅₀ (pM)	450	210
GT1b EC ₅₀ (pM)	5	9

favorable PK properties in dog as well as a very low clearance, a 5.29 h half-life and 35% oral bioavailability in rat (Table 4).

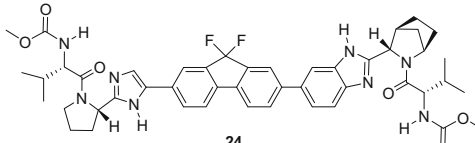
We sought to incorporate this pharmacokinetic enhancing azabicyclo[2.2.1] ring system into our unsymmetric imidazole/benzimidazole series. In this process we discovered a further important facet of structure-activity relationships in the unsymmetric core series. Earlier we found that the directionality of the central portion of the core (phenyl-alkyne) relative to the unsymmetric imidazole/benzimidazole groups produced a matched and mismatched pairing (compounds **11** and **12**). This core directionality again provided a matched and mismatched pairing but this time with positioning of the terminal azabicyclo[2.2.1] ring system relative to the unsymmetric core (i.e., positioning of the azabicyclo[2.2.1] system on either end of the core). When the bicyclic ring system is proximal to the benzimidazole (**22**), the inhibitor is more potent than when the bicyclic ring system is proximal to the imidazole (**23**) (Fig. 7). Further, the matched case inhibitor is more potent (**22**, GT1a = 160 pM) than the azabicyclic symmetric inhibitor (**21**, GT1a = 210 pM, Table 5), while the mismatched case inhibitor **23** is less potent (GT1a = 660 pM) than the symmetric case **21**. These results highlight a critical discovery; unsymmetric cores allow for diversification of structure that can provide beneficial properties (matched cases, with beneficial properties such as enhanced potency and/or pharmacokinetics) over the more limited symmetric cases. Finally, we had sought to determine if the beneficial PK properties imparted by the azabicyclo[2.2.1] ring in symmetric inhibitor **21** might translate in the unsymmetric series. Indeed, the half-lives in rat and dog are improved in azabicyclo[2.2.1] inhibitor **22** (unsymmetric “matched case”) over the corresponding pyrrolidine **14** (Table 4).

Having improved the PK half-life with azabicyclic inhibitor **22**, we sought to enhance its potency. As demonstrated earlier, fused-ring systems within the inhibitor’s core can provide potency enhancements. Accordingly, incorporation of the



	22	23
GT1a EC ₅₀ (pM)	160	660
GT1b EC ₅₀ (pM)	6	21

Fig. 7 Differential end-substitution with an unsymmetric core leads to divergence in potency. Bridged azabicyclic ring system is more potent on benzimidazole side of the core



GT1a EC ₅₀ (pM)	56
Protein-binding adjusted	784

Fig. 8 Difluorofluorene core improves potency in combination with azabicyclic pyrrolidine

difluorofluorene ring system in inhibitor **24** (Fig. 8) afforded a GT1a potency of 56 pM, which is an ~3fold improvement over the biaryl core inhibitor **22**.

The inhibitors described herein are highly protein bound, even in the replicon cellular assay which includes 10% fetal bovine serum (FBS). We utilize a dialysis methodology to assess relative inhibitor free fraction based on plasma protein binding and then generate a value for the protein-binding-adjusted potency. In this method, the inhibitor of interest is dialyzed between 100% human plasma in one well and replicon cell culture medium (including 10% FBS) in a second well [22]. The measured concentration ratio between wells can be multiplied by the replicon potency to “cancel” the cell culture medium binding and provide a human plasma protein-binding-adjusted potency (PA EC₅₀). This methodology affords a GT1a PA EC₅₀ for inhibitor **24** of 784 pM. We sought to improve upon this protein-binding-adjusted potency.

3 Ledipasvir (1, LDV, GS-5885)

During our final phase of discovery, one of the directions we undertook was modification of the pyrrolidine of inhibitor **24**. Incorporation of a spirocyclopropyl ring provided the most potent inhibitor (compound **1**) in the series with improvements in both the replicon potency and the plasma protein-binding-adjusted potency (GT1a EC₅₀ = 31 pM, PA EC₅₀ = 208 pM, Fig. 9) over inhibitor **24**; interestingly, the PA EC₅₀ of **1** versus **24** was differentially improved (3.6-fold, 208 versus 740 pM) relative to the EC₅₀ (1.8-fold, 31 versus 56 pM). The protein-binding ratio of human plasma versus cell culture medium of 6.7-fold for inhibitor **1** as

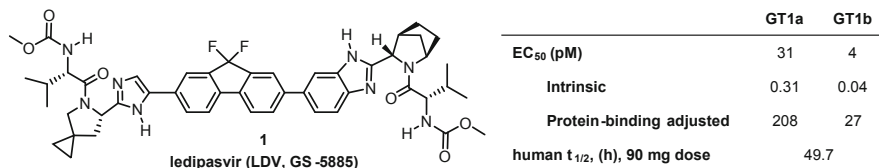


Fig. 9 Ledipasvir structure, replicon cellular antiviral potency, intrinsic replicon potency, and human PK half-life

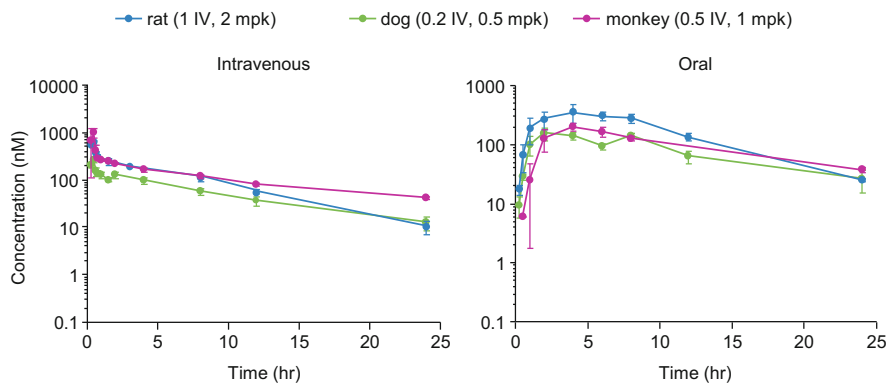


Fig. 10 Pharmacokinetic curves for ledipasvir (**1**) in rat, dog, and cynomolgus monkey. LDV has long half-lives in preclinical species

measured by dialysis was the lowest for any advanced inhibitor we had assessed. Compound **1** is highly protein bound, with only 1% free drug even in the replicon cell culture medium (containing 10% fetal bovine serum). Accounting for free drug, the intrinsic replicon GT1a and GT1b EC₅₀ values for compound **1** are 310 femtomolar (fM) and 40 fM, respectively (Fig. 9).

Pharmacokinetic curves and PK parameters for inhibitor **1** are found in Fig. 10 and Table 6. Compound **1** has the longest half-lives (from 4.7 to 10.3 h in rat, dog, and monkey) among the compounds described herein and has high metabolic stability across preclinical species. Based on its exceptional replicon and PA potency, excellent pharmacokinetic half-lives, bioavailability, and low predicted clearance, compound **1** was selected for development and is now known as ledipasvir (LDV, GS-5885).

A synthesis of LDV is depicted in Scheme 1. The azabicyclo[2.2.1] ester **1a** [23] is debenzylated with palladium hydroxide and hydrogen, Boc protected, and the ester hydrolyzed to form bicyclic acid **1b**. Coupling of **1b** with 4-bromo-1,2-diaminobenzene and heating in ethanol affords benzimidazole **1c**, which is borylated to form pinacol boronate ester **1d**. Bromo-iodofluorene **1e** is difluorinated in a mild and novel “one-pot” procedure by treatment with *N*-fluorobenzenesulfonimide followed by KHDMS in THF (**1f**). The Grignard of **1f** is selectively formed and

Table 6 In vitro and in vivo PK parameters for ledipasvir in preclinical species and humans

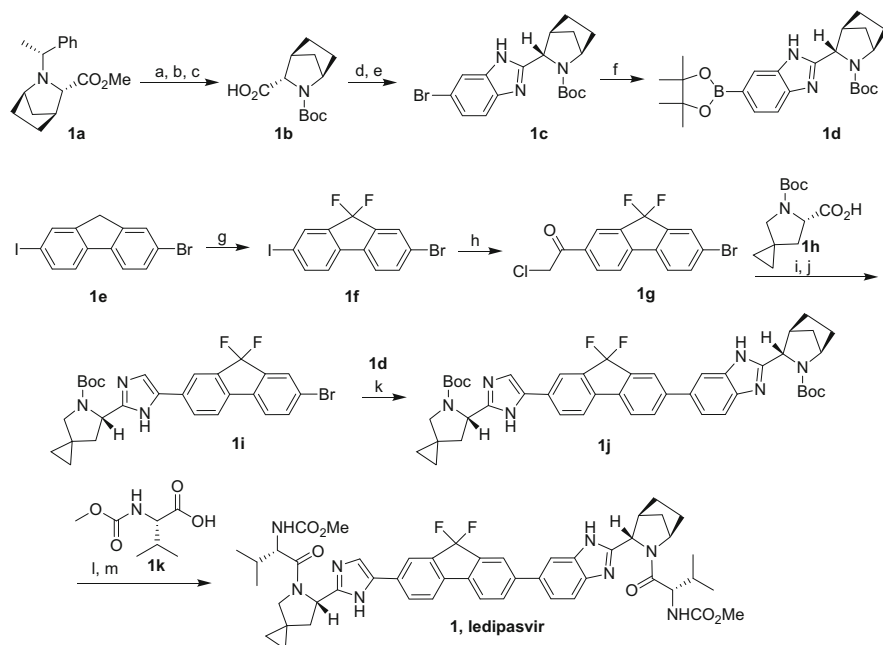
Species	Dose (route)	In vitro		In vivo				
		Percent free in plasma (%)	Pred CL microsomes (L/h/kg)	$t_{1/2}$ (h) ^a	CL (L h ⁻¹ kg ⁻¹) ^a	V_{ss} (L kg ⁻¹) ^a	MRT ^b (h)	%F
SD rat	1 mpk ^c (IV)	0.19	<0.34	4.67 ± 0.56	0.43 ± 0.04	2.66 ± 0.13	6.19 ± 0.28	32.5 ± 6.7
Beagle dog	0.2 mpk ^c (IV)	0.06	<0.18	7.41 ± 0.80	0.13 ± 0.02	1.19 ± 0.13	9.20 ± 1.35	53.0 ± 12.4
Cyno monkey	0.5 mpk ^c (IV)	3.85	<0.17	10.3 ± 1.2	0.17 ± 0.00	2.15 ± 0.42	12.9 ± 2.1	41.1 ± 3.6
Human	90 mg (PO) ^d	0.68	0.012 ^e	49.7 ^d	–	–	–	~50% ^{d,f}

^aCL, V_{ss} , MRT, and $t_{1/2}$ are from IV dosing^bMean residence time^cmpk = milligrams per kilogram^dData in HCV-infected patients at approved dose in Harvoni[®]; see Tables 8 and 9 for results from other doses in humans^eMeasured in human hepatocytes using ³H-ledipasvir^fHuman bioavailability estimated from CL/F from HCV-infected patients and CL predicted from preclinical studies

reacted with 2-chloro-*N*-methoxy-*N*-methylacetamide to generate the chloroketone **1g** which is alkylated with the potassium salt of spirocyclic acid **1h**. Heating of the resulting keto-ester with ammonium acetate in toluene affords cyclization to difluorofluorene-imidazole **1i**. Coupling of pinacol boronate **1d** with bromo-fluorene **1i** completes the core of ledipasvir **1j**. Double Boc deprotection of **1j** and HATU-mediated coupling with Moc-valine (**1k**) affords ledipasvir, **1** [14].

Further data supporting the decision to undertake the clinical development of ledipasvir follows. LDV showed no measurable instability at the lower limit of detection in our in vitro liver microsome assays in preclinical species and human (human predicted CL <0.16 L/h/kg). Therefore ³H-LDV was incubated in hepatocytes to measure low-level metabolites for calculation of the predicted CL. This approach afforded an exceptionally low predicted human metabolic clearance of 0.012 L/h/kg (Table 6). In bile duct-cannulated dogs, LDV was slowly excreted, and over 24 h 65% of the dose was recovered as parent drug in bile consistent with the low hepatic oxidative metabolism measured across species in microsomes and human hepatocytes. (Less than 1% of LDV was recovered in urine.)

Despite its high protein binding, LDV displays moderate volumes of distribution (V_{ss}). It is interesting to note that although high serum protein binding often leads to a low volume of distribution [24], the V_{ss} of LDV in preclinical species (1.2–2.7 L/h/kg) is significantly higher than the plasma volume. The moderate V_{ss} of LDV in concert with its high metabolic stability contributes to its long PK half-life. As a consequence of its low oxidative metabolism in human hepatocytes, moderate V_{ss} in rat, dog, and monkey, and slow biliary excretion in dog, LDV was predicted to have a long human half-life. Based on its PK and potency, LDV was predicted to have a sufficiently low once-daily dose that would be compatible with dosing in a single-tablet regimen. As a result, LDV was progressed into clinical development. In our discovery of LDV, we targeted a long human half-life to



Scheme 1 ledipasvir synthesis. (a) Pd(OH)₂/C, H₂, EtOH; (b) Boc₂O, *i*-Pr₂NEt, CH₂Cl₂; (c) LiOH, THF/MeOH/H₂O; (d) 4-bromo-1,2-diaminobenzene, HATU, 4-methylmorpholine, DMF; (e) EtOH; (f) bis(pinacolato)diboron, PdCl₂(dppf)₂, KOAc, 1,4-dioxane; (g) *N*-fluorobenzenesulfonimide, KHMDS, THF; (h) *i*-PrMgCl, 2-chloro-*N*-methoxy-*N*-methylacetamide, THF; (i) **1h**, K₂CO₃, KI, acetone; (j) NH₄OAc, PhMe; (k) **1d**, Pd(OAc)₂, PPh₃, NaHCO₃, DME/H₂O; (l) HCl/dioxane/DCM; (m) **1k**, HATU, *i*-Pr₂NEt, DMF

enable once-daily dosing in an STR and to ensure that drug trough concentrations would remain sufficiently high to suppress viral breakthrough and the emergence of resistance potentially even in the event of patient non-compliance.

As described herein, multiple unique motifs make up the complex structure of ledipasvir and contribute to its picomolar cellular and PA potency, high metabolic stability, and excellent pharmacokinetic properties. The structure of LDV has captured the interest of a number of authors and has been cited in a range of publications focusing on some of the intriguing structural elements now becoming utilized in medicinal chemistry, including benzimidazoles [25]; spirocyclic ring systems [26]; cyclopropanes [27], bridged heterocyclic ring systems [28]; incorporation of stereocenters (LDV has six) [29]; and the use of fluorine in drug discovery (whereas most fluorinated drugs include aryl or heteroaryl fluorides, few bear aliphatic fluorine substitution as in LDV) [30]. With these and other elements taken together, the unique structure of ledipasvir is highly complex within known drug space. In a recent publication detailing a computational algorithm that defines structural complexity in drugs, ledipasvir is the most structurally complex orally bioavailable drug among the examples discussed [31]. The chemical complexity of ledipasvir based on

Table 7 Ledipasvir is not compliant with most contemporary medicinal chemistry rule-based bioavailability and “drug-likeness” metrics

Rule set	Parameter	Rule limit value	LDV value
Lipinski rule of 5 [36]	Molecular weight	≤ 500	889
Lipinski rule of 5	CLogP ^a	≤ 5	6.71
Lipinski rule of 5	H-bond donors	≤ 5	4
Lipinski rule of 5	H-bond acceptors ^b	≤ 10	14
Veber [37]	Rotatable bonds ^c	≤ 10	12
Veber	Polar surface area ^c	$< 140 \text{ \AA}^2$	174 \AA^2
Ring rule [38]	# of rings	≤ 5 is 95th percentile	10
Aromatic ring rule [39]	# Aromatic rings	≤ 3	5

^aChemBioDraw 14.0, CambridgeSoft Corporation^bSum of N's and O's as defined by Lipinski et al. [36]^cPipeline pilot

ring structure and calculated properties defines it as a “rulebreaker” drug by multiple metrics. LDV has been discussed in drugs “beyond the rule of 5” (bRo5) [32, 33], bRo5 “chameleonic” drugs [34] that display differential lipophilicity based on their conformational state, and has been provided as an example of the importance of organic synthesis in drug discovery [35].

Our discovery and implementation of the structural motifs incorporated in LDV followed a data-driven path that sought improvement of measured properties such as antiviral activity and in vitro and in vivo pharmacokinetic attributes and disregarded rule-based metrics. Indeed ledipasvir is a “rulebreaker” compound that defies much of the dogma dominating contemporary medicinal chemistry design that attempts to define “drug likeness” and potential for bioavailability. Rule limit values for molecular weight, calculated logP, the number of H-bond donors and acceptors [36], the number of rotatable bonds and polar surface area [37], the number of ring structures [38], and the number of aromatic rings [39] are provided in Table 7, along with the corresponding values for LDV. These rule-based metrics are provided here for reference and were not utilized in any way during the discovery of LDV. LDV lies outside most of these metric-based rules. Ledipasvir has proven to be a bioavailable, efficacious, safe, and well-tolerated drug.

4 Translation of Ledipasvir’s Preclinical Potency and PK Properties in Phase 1 Clinical Trials

The preclinical pharmacokinetic optimization efforts in the discovery of LDV proved fruitful. In human healthy volunteers the exposure of a single dose of LDV increases dose proportionally from 3 to 100 mg, and gratifyingly the half-lives are typically over 40 h (Fig. 11 and Table 8) [14]. The LDV 24 h trough drug concentration is well over the PA EC₅₀ at all doses (depicted with the red dotted line, Fig. 11), ranging from 12-fold at the 3 mg dose to 470-fold at the 100 mg dose.

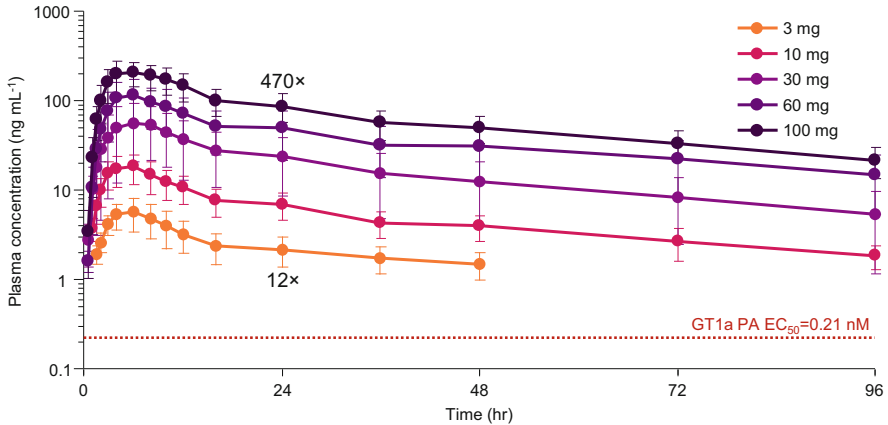


Fig. 11 LDV single oral dose pharmacokinetics in healthy volunteers

Table 8 LDV PK parameters after single oral dose administration, eight healthy volunteers per cohort

Mean parameter (%CV)	LDV oral dose				
	3 mg	10 mg	30 mg	60 mg	100 mg
$t_{1/2}$ (h)	45.2 (51)	42.4 (29)	37.2 (32)	44.2 (22)	39.5 (23)
C_{max} (nM)	6.75 (37)	21.3 (36)	82.2 (51)	133 (50)	242 (35)
AUC_{inf} (nM h)	245 (60.6)	695 (32.3)	2,717 (60.3)	5,299 (58.2)	8,658 (34.3)
C_{24hr} (nM)	2.45 (37)	7.94 (34)	31.4 (60)	56.4 (57)	98.8 (35)

For the 10–100 mg doses, the trough concentrations remain well over the PA EC_{50} even at 96 h post-dose.

The PK curves and PK parameters post the third-daily dose of LDV administered to GT1 HCV-infected individuals are depicted in Fig. 12 and Table 9, respectively [40]. Here the exposures are approximately dose proportional over five dose levels from 1 to 90 mg, and the half-life for the 90 mg dose of LDV (the dose utilized in the LDV/SOF STR Harvoni[®]) is 49.7 h. Although not yet at steady state 24 h post the third dose, the drug concentration is 610-fold over the GT1a PA EC_{50} and 4,730-fold over the GT1b PA EC_{50} . The 24 h drug concentration is above the GT1a PA EC_{50} even for the lowest total dose of 1 mg.

Accordingly, all monotherapy doses of LDV from 1 to 90 mgs displayed potent and rapid viral load reductions (VLR) in GT1-infected individuals (Fig. 13) [40]. Doses 3 mg and higher rapidly achieved VLR ~ 3 log₁₀ within 24 h post the first dose and exceeded 3 log₁₀ mean maximal viral load reductions during the dosing interval. Even the 1 mg total dose afforded a mean maximal VLR of 2.3 log₁₀. The 30 and 90 mg doses maintained >2 log₁₀ viral suppression at 144 h (4 days post the third and final dose), while the 10 mg dose in GT1b-infected

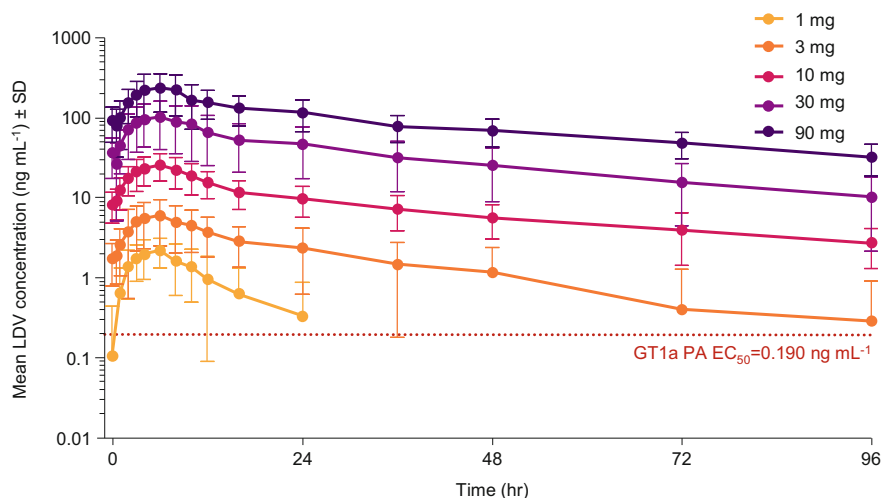


Fig. 12 LDV PK in patients post the third and final dose. Depicted as mean with standard deviation. Day 3 dose administered at time zero

Table 9 LDV pharmacokinetic parameters post third dose in HCV GT1-infected patients

	LDV oral dose				
	1 mg	3 mg	10 mg	30 mg	90 mg
$t_{1/2}$ (h)	13.0 (7.7, 17.8)	22.8 (13.1, 36.8)	39.9 (28.5, 47.2)	41.7 (25.8, 53.4)	49.7 (37.8, 54.3)
C_{max} (ng mL ⁻¹)	2.2 (39.7)	6.1 (56.6)	25.3 (40.0)	103.3 (57.5)	247.7 (45.4)
C_{tau} (ng mL ⁻¹)	0.3 (161.0)	2.4 (73.6)	9.7 (41.5)	46.5 (62.7)	115.9 (42.6)
AUC_{tau} (ng h mL ⁻¹)	34.0 (29.8)	89.7 (54.6)	368.8 (39.0)	1,592.4 (59.5)	3,815.5 (42.1)

Data are presented as mean values (coefficient of variability %); $t_{1/2}$ are median (quartile 1, quartile 3); Tau values are at 24 h post-dose; 10 mg cohort ($n = 19$) includes GT1a,b patients, others are GT1a ($n = 10$)

individuals afforded a mean maximal VLR of 3.3 log₁₀ and maintained ~2.5 log₁₀ viral suppression 4 days post the final dose.

The NS5B polymerase is highly error-prone. Based on the polymerase error rate, the HCV replication rate in vivo (10^{12} viral particles per day per patient), and the size of the HCV genome, it is estimated that every single, double, and some triple viral mutants are produced every day in a single patient [41]. In the NS5A gene sequence, variants present at gene positions 28, 30, 31, and 93 have shown reduced susceptibility to inhibitors [42]. Substitutions in the NS5A sequence are termed resistance-associated substitutions (RAS, plural RASs) and noted with the amino acid in the wild-type (WT) sequence first, the position next, and substituted amino acid last;

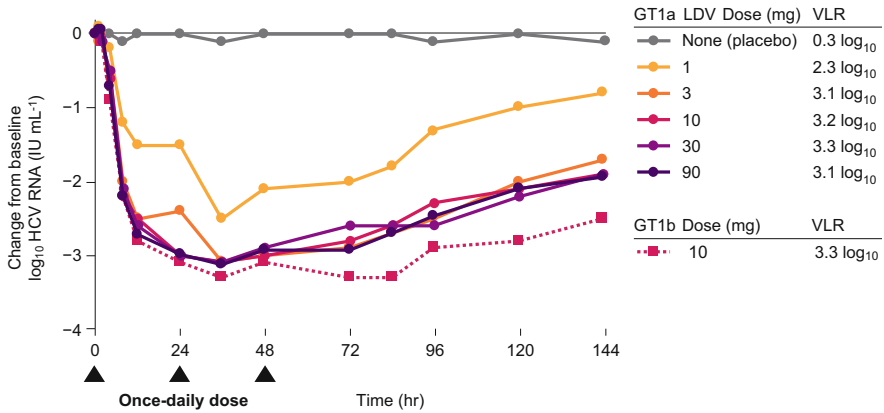


Fig. 13 Viral load reduction, 3-day LDV dosing in monotherapy in GT1a (1–90 mg) or GT1b patients (10 mg). All cohorts included ten patients except the GT1a 10 mg dose (9) and the placebo (11)

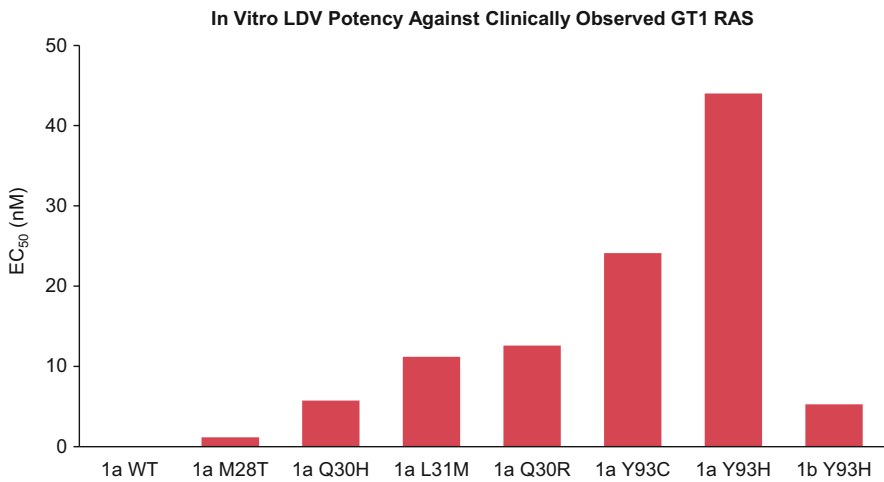


Fig. 14 Ledipasvir potency against clinically observed GT1 RAS (transient transfection in wild-type replicon)

e.g., Y93H denotes the RAS where a histidine is substituted for the WT tyrosine at position 93. Figure 14 and Table 10 depict the potency of LDV for a range of GT1a and GT1b RASs [43]. These RASs are present at low levels in most patients prior to treatment, but in some cases one or more RASs may be present at higher levels or may even represent dominant virus. The mean maximal viral load reduction for a given patient in monotherapy is defined by the titer of viruses with these RASs along with the inhibitor activity against these RASs.

It is interesting to note that there does not appear to be a dose-response for LDV in monotherapy for doses from 3 to 90 mg in the Phase 1b monotherapy study shown in Fig. 13 (VLR ranges from 3.1 to 3.3 log₁₀ over this dose range) [40]. Assessment of baseline RASs helps to understand the apparent absence of dose-response. By chance, RASs were not present (at detectable levels) in any patient at baseline in the 1 and 3 mg GT1a cohorts (Fig. 15, baseline RAS assessments were determined post cohort randomization) [42]. Thus the patients in the 1 and 3 mg dosing cohorts had a disproportionately strong mean responses relative to the 30 and 90 mg cohorts which had relatively weaker responses in two patients showing high levels of the RAS Q30E/Q (30 mg cohort) or L31M (90 mg cohort). The weaker response of LDV against these RASs in vivo is consistent with the reduced susceptibility of the L31M and Q30E replicons to LDV in vitro (Table 10, Fig. 14). In our work to

Table 10 GT1 resistance profile of ledipasvir against clinically relevant resistance-associated substitutions (RAS)

	GT1a EC ₅₀ (nM)								GT1b EC ₅₀ (nM)	
	WT	M28T	Q30H	Q30R	L31M	Y93C	Q30E	Y93H	WT	Y93H
LDV	0.031	1.9	5.7	19.6	17	49.6	169	52.0	0.004	7.2

All RASs are transiently transfected GT1a or GT1b subgenomic HCV replicons

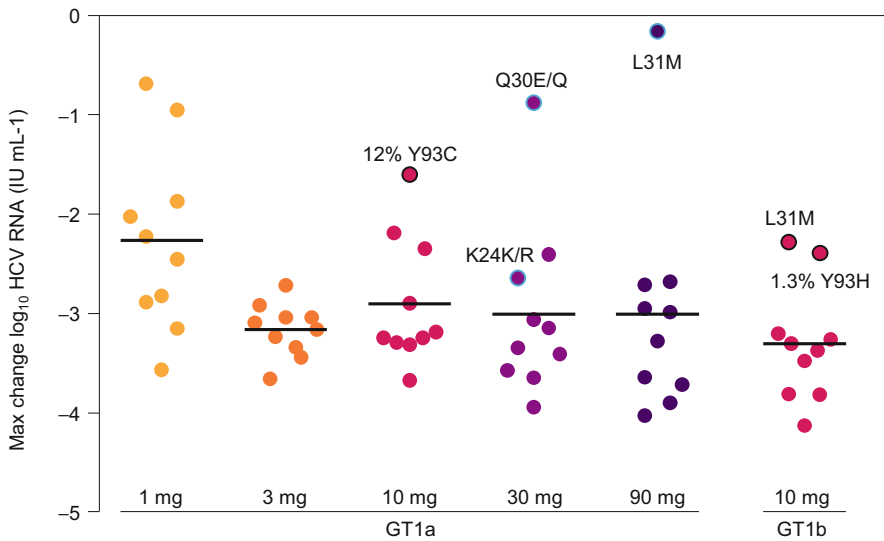


Fig. 15 LDV clinical VLR by individual patient. Clinical RASs found at baseline are noted. RASs are measured by two methods, either by population sequencing (detectable as >25% of total viral population which are labeled and outlined in blue) or by deep sequencing (limit of detection ~1% of total population are labeled and outlined in black). The percentage of the resistant population is noted for RAS detected by deep sequencing. The horizontal lines represent the mean viral load reduction

discover a pan-genotypic NS5A inhibitor, we improved activity across genotypes along with improved potency against NS5A RASs. The culmination of those efforts resulted in the discovery of velpatasvir [15–17], a potent pan-genotypic NS5A inhibitor with a high barrier to resistance that is combined with sofosbuvir in the first pan-genotypic STR Epclusa[®] and with sofosbuvir and voxilaprevir in the pan-genotypic STR Vosevi[®]. For both Harvoni[®] and Epclusa[®], the presence of RASs detected in patients at baseline does not diminish the SVR relative to the SVR in patients with no detectible RASs [16, 44–48].

5 LDV/SOF Approval and Real-World Data

In October of 2014 LDV (90 mg) combined with sofosbuvir (400 mg) was approved under the name Harvoni[®], for the treatment of GT1 HCV-infected non-cirrhotic and compensated cirrhotic patients based on the ION 1–4 Phase 3 clinical trials [44–47]. Administration of a single pill, once-daily for 8 or 12 weeks affords cure rates from 94 to 97%. In subsequent studies, Harvoni[®] was shown to afford high SVR rates in genotype 4, 5, and 6 patients (LDV displays potent GT4a–6a replicon potency, Table 1), and the prescribing label was accordingly expanded for treatment of these patients (https://www.accessdata.fda.gov/drugsatfda_docs/label/2015/205834s001lbl.pdf. Accessed 10 June 2018) [5].

A measure of the practicality of a treatment regimen can be assessed by studies outside of the controlled environment of clinical trials in “real-world” “effectiveness” studies. There is no more extreme disparity between efficacy (risk-benefit in a clinical setting) in Phase 3 trials and real-world effectiveness (risk-benefit in real-world healthcare practice) than has been observed for SVR rates for IFN-based regimens. The poor tolerability, high complexity, and low efficacy of IFN-based therapy all conspire to afford real-world SVR rates that are dramatically lower than the ~60% [49, 50] achieved in later Phase 3 clinical studies. Strikingly, the real-world SVR in the US Veterans Administration (VA) is as low as 3.5%, with only 35.9% of the 99,156 HCV-infected veterans having no contraindications to this poorly tolerated regimen [51]. The attrition leading to this low SVR rate is outlined in Fig. 16 and includes patients unable or unwilling to undergo treatment, patients unable to complete treatment, and a high failure rate for those completing treatment. In contrast, a recent study of Harvoni[®] in this US VA HCV-infected patient population showed that 90% of patients had no contraindications, and of those patients initiating therapy the real-world SVR was 92–94% (4,365 patients, 8- and 12-week regimens, respectively). The high SVR of SOF/LDV in this population is even more notable since the authors of the study posited that advanced age, higher body mass index, ethnicity, and the prevalence of advanced liver disease (fibrosis and cirrhosis, including decompensated cirrhosis) are all factors defining this VA population as more difficult to treat than a typical cohort of HCV-infected individuals [51]. Accordingly, elimination of HCV within the 200,000 US VA HCV-infected individuals is projected for the end of the year 2018 [52].

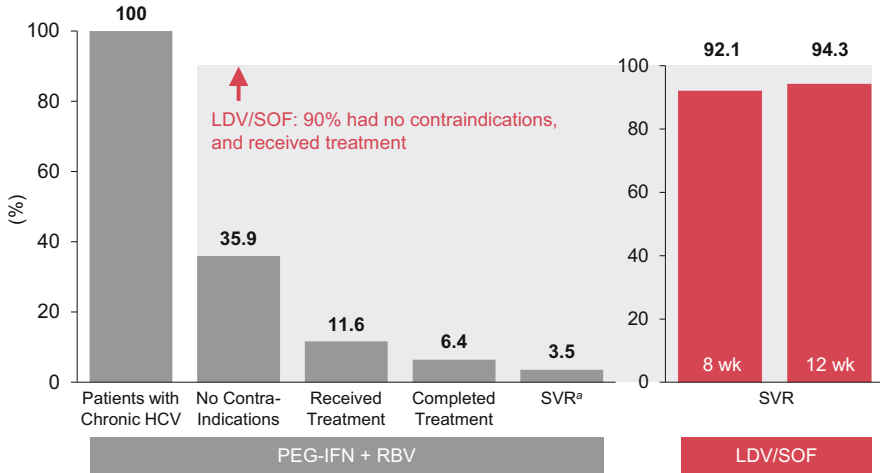


Fig. 16 Real-world SVR rates in the US Veterans Administration: IFN-based effectiveness contrasted with LDV/SOF. Tolerability and simplicity of LDV/SOF therapy present a striking real-world effectiveness advantage over IFN-based therapies. ^aVA calculated IFN-based SVR by including attrition from contraindications and those who did not receive treatment

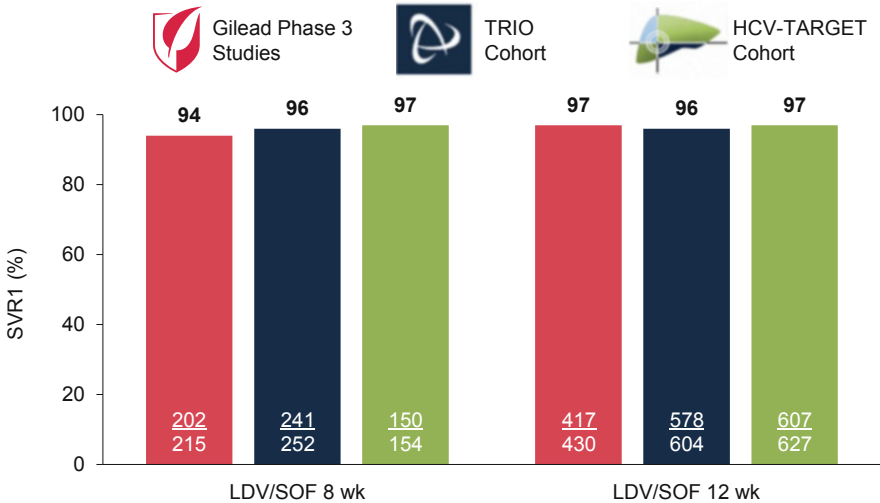


Fig. 17 Comparison of overall SVR rates from Phase 3 clinical studies relative to “real-world” studies (treatment-naïve patients). Bars colored as follows: red = Gilead Phase 3 clinical studies; dark blue = Trio Real-World Cohort; green = HCV Target Real-World Cohort

Additionally, two large real-world cohorts showed comparable results to those of the LDV/SOF Phase 3 ION-1 and ION-3 clinical trials as depicted in Fig. 17 ranging from 94 to 97% SVR. The Hepatitis C Therapeutic Registry and Research Network (HCV-TARGET) is a study comprised of North American and European academic

and community medical centers. Trio Health Innervation Platform (TRIO) is a disease management cloud-based platform with data collection from specialty pharmacies [53]. It is probable that the simplicity, safety, and potency of the SOF/LDV single-tablet regimen are important attributes leading to this high level of translation from clinical trials to the real world [54].

6 Conclusion

Ledipasvir is a highly potent NS5A (GT1a and GT1b EC_{50} values are 31 and 4 pM, respectively) inhibitor with a long pharmacokinetic half-life of 49.7 h in HCV-infected individuals. These attributes were critical aspects of the discovery LDV, making it a drug favorable for combination in a single-tablet regimen. Ledipasvir is the first FDA-approved NS5A inhibitor (October 10, 2014). LDV combined with sofosbuvir as Harvoni[®] is the first STR for the treatment and cure of HCV infection and the first HCV therapy to provide cure rates of 94–97% in as little as 8 weeks of treatment. Subsequent to approval for GT1 HCV infection, the label of Harvoni[®] was expanded to include treatment of GT4–6-infected individuals. The real-world effectiveness of Harvoni[®] is comparable to that achieved in controlled clinical trials, making it a valuable regimen for application in resource-limited settings and an important drug for HCV eradication programs [51, 52].

Acknowledgment The author would like to thank the Gilead research and development colleagues that discovered and developed ledipasvir and the clinical collaborators and patients who made this work possible.

Compliance with Ethical Standards

Conflict of Interest: John O. Link is an employee of Gilead Sciences, Inc.

Ethical Approval: All procedures performed in studies involving human participants were in accordance with the ethical standards of the institutional and/or national research committee and with the 1964 Helsinki declaration and its later amendments or comparable ethical standards.

Informed Consent: Informed consent was obtained from all individual participants included in the study.

References

1. Moon AM, Green PK, Berry K, Ionnu GN (2017) *Aliment Pharmacol Ther* 45:1201–1212
2. North CS, Hong BA, Adewuyi SA, Pollio DE, Jain MK, Devereaux R, Quarley NA, Ashitey S, Lee WM, Lisker-Melman M (2012) *General Hosp Psychiatry* 35:122
3. Ly KN, Hughes EM, Jiles RB, Holmberg SD (2016) *Clin Infect Dis* 62:1287
4. Sofia M (2015) *J Med Chem Rev* 50:397
5. Sofia MJ, Link JO (2017) In: Chackalamannil S, Rotella D, Ward S (eds) *Comprehensive medicinal chemistry III*. Elsevier, Amsterdam, p 558

6. Weisman R (2018) Boston Globe, Vertex to stop selling hepatitis C drug Incivek. <https://www.bostonglobe.com/business/2014/08/12/vertex-stop-selling-hepatitis-drug-incivek/EI0jtOpH9I1CaIgQpSUKWO/story.html>. Accessed 19 June 2018
7. Palmer E FiercePharma, Vertex's Incivek unseats Celebrex as fastest drug launch ever. <https://www.fiercepharma.com/sales-and-marketing/vertex-s-incivek-unseats-celebrex-as-fastest-drug-launch-ever>. Accessed 10 June 2018
8. Herper M, Forbes (2014) The top drug launches of all time. <https://www.forbes.com/sites/matthewherper/2015/07/29/the-top-drug-launches-of-all-time/#6fe13a386512>. Accessed 19 June 2018
9. EP Vantage (2018) The biggest drug launches – hep C dominates but Tecfidera stands out. <http://www.epvantage.com/Universal/View.aspx?type=Story&id=766560&isEPVantage=yes>. Accessed 21 June 2018
10. Hebner CM, Han B, Brendza KM, Nash M, Sulfab M, Tian Y, Hung M, Fung W, Vivian RW, Trenkle J, Taylor J, Bjornson K, Bondy S, Liu X, Link J, Neyts J, Sakowicz R, Zhong W, Tang H, Schmitz U (2012) PLoS One 7(6):e39163
11. Sheng XC, Casarez A, Cai R, Clarke MO, Chen X, Cho A, Delaney III WE, Doerfler E, Ji M, Mertzman M, Pakdaman R, Pyun HJ, Rowe T, Wu Q, Xu J, Kim CU (2012) Bioorg Med Chem Lett 22(3):1394–1396
12. Sheng X, Appleby T, Butler T, Cai R, Chen X, Cho A, Clarke MO, Cottell J, Delaney IV WE, Doerfler E, Link J, Ji M, Pakdaman R, Pyun HJ, Wu Q, Xu J, Kim CU (2011) Bioorg Med Chem Lett 22(7):2629–2634
13. Magiorkinis G, Sypsa V, Magiorkinis E, Paraskevis D, Katsoulidou A, Belshaw R, Fraser C, Pybus OG, Hatzakis A (2013) PLoS Comput Biol 9(1):e1002876
14. Link JO, Taylor JG, Xu L, Mitchell M, Guo H, Liu H, Kato D, Kirschberg T, Sun J, Squires N, Parrish J, Keller T, Yang ZY, Yang C, Matles M, Wang Y, Wang K, Cheng G, Tian Y, Mogalian E, Mondou E, Cornpropst M, Perry J, Desai MC (2014) J Med Chem 57:2033
15. Link JO, Taylor JG, Trejo-Martin TA, Kato D, Katana AA, Krygowski ES, Yang Z-Y, Zipfel S, Cottell JJ, Bacon EM, Tran CV, Yang CY, Wang Y, Wang K, Zhao G, Cheng G, Tian Y, Gong R, Lee J, Yu M, Gorman E, Mogalian E, Perry J. Bioorg Med Chem Lett. Submitted
16. Link JO (2018) Med Chem Rev 53:541–564
17. Bacon EM, Cottell JJ, Katana AA, Kato D, Krygowski ES, Link JO, Taylor J, Tran CV, Trejo-Martin TA, Yang Z-Y, Zipfel S (2012) Patent application WO 2012/068234 A2
18. Taylor JG, Zipfel S, Ramey K, Vivian R, Schrier A, Karki KK, Katana A, Kato D, Kobayashi T, Martinez R, Sangi M, Siegel D, Tran CV, Yang Z-Y, Zablocki J, Yang CY, Wang Y, Wang K, Chan K, Barauskas O, Cheng G, Jin D, Schultz B, Appleby T, Villasenor A, Link JO. Bioorg Med Chem Lett. Submitted
19. Porter DP, Guyer B (2013) In: Desai MC, Meanwell NA (eds) Successful strategies for the discovery of antiviral drugs. The Royal Society of Chemistry, Cambridge, p 482
20. Blanco JL, Montaner JS, Marconi VC, Santoro MM, Campos-Loza AE, Shafer RW, Miller MD, Paredes R, Harrigan R, Nguyen ML, Perno CF, Gonzalez-Hernandez LA, Gatell JM (2014) AIDS 28:2531–2539
21. Guo H, Kato D, Kirschberg TA, Liu H, Link JO, Mitchell ML, Parrish JP, Squires N, Sun J, Taylor J, Bacon EM, Canales E, Cho A, Cottell JJ, Desai M, Halcomb RL, Krygowski ES, Lazerwith SE, Mackman R, Pyun HJ, Saugier JH, Trenkle J, Tse W, Vivian RW, Schroeder SD, Watkins WJ, Xu L, Yang Z-Y, Kellar T, Sheng X, Clarke M, O'Neil H, Chou C-H, Graupe M, Jin H, McFadden R, Mish M, Metobo R, Phillips BW, Venkataramani C (2010) Patent application WO 2010/132601 A1
22. Mo H, Yang C, Wang K, Wang Y, Huang M, Murray B, Qi X, Sun SC, Deshpande M, Rhodes G, Miller MD (2011) J Viral Hepat 18:338
23. Stella L, Abraham H, Feneau-Dupont J, Tinant B, Declercq JP (1990) Tetrahedron Lett 31 (18):2603–2606
24. Bruno LB, Agrawal VK (2014) Interdiscip Sci Comput Life Sci 6:71–83
25. Akhtar W, Khan MF, Verma G, Shaquiquzzaman M, Rizvi MA, Mehdi SH, Akhter M, Alam MM (2017) Eur J Med Chem 126:705–753
26. Zheng Y, Tice CM, Singh SB (2014) Bioorg Med Chem Lett 16:3673–3682

27. Talele TT (2016) *J Med Chem* 59:8712–8756
28. Degorce SL, Bodnarchuk MS, Cumming IA, Scott JS (2018) *J Med Chem* 61:8934–8943
29. Singh K, Shakya P, Kumar A, Alok S, Kamal M, Singh SP (2014) *Int J Pharm Sci Res* 5:4644–4659
30. Zhou Y, Wang J, Gu Z, Wang S, Zhu W, Aceña JL, Soloshonok VA, Izawa K, Liu H (2016) *Chem Rev* 116:422–518
31. Proudfoot JR (2017) *Bioorg Med Chem Lett* 27:2014–2017
32. Doak BC, Over B, Giordanetto F, Kihlberg J (2014) *Chem Biol* 21:1115–1142
33. DeGoey DA, Chen HJ, Cox PB, Wendt MD (2018) *J Med Chem* 12:2636–2651
34. Rossi SM, Doak BC, Backlund M, Poongavanam V, Over B, Ermondi G, Caron G, Matsson P, Kihlberg J (2018) *J Med Chem* 61:4189–4202
35. Rotella DP (2016) *ACS Chem Neurosci* 7:1315–1316
36. Lipinski CA, Lombardo F, Dominy BW, Feeney PJ (1997) *Adv Drug Deliv Rev* 23:3
37. Veber DF, Johnson SR, Cheng HY, Smith BR, Ward KW, Kopple KD (2002) *J Med Chem* 45:2615
38. Taylor RD, MacCoss M, Lawson AD (2014) *J Med Chem* 57:5845
39. Ritchie TJ, Macdonald SJ (2009) *Drug Discov Today* 14:1011
40. Lawitz EJ, Gruener D, Hill JM, Marbury T, Moorehead L, Mathias A, Cheng G, Link JO, Wong KA, Mo H, McHutchison JG, Brainard DM (2012) *J Hepatol* 57:24–31
41. Nguyen T, Guedj J (2015) *CPT Pharmacometrics Syst Pharmacol* 4:231
42. Wong KA, Worth A, Martin R, Svarovskaia E, Brainard DM, Lawitz E, Miller MD, Mo H (2013) *Antimicrob Agents Chemother* 57(12):6333–6340
43. Cheng G, Tian Y, Doehle B, Peng B, Corsa A, Lee YJ, Gong R, Yu M, Han B, Xu S, Dvory-Sobol H, Perron M, Xu Y, Mo H, Pagratis N, Link JO, Delaney W (2016) *Antimicrob Agents Chemother* 60(3):1847–1853
44. Afdhal N, Zeuzem S, Kwo P, Chojkier M, Gitlin N, Puoti M, Romero-Gomez M, Zarski JP, Agarwal K, Buggisch P, Foster GR, Bräu N, Buti M, Jacobson IM, Subramanian GM, Ding X, Mo H, Yang JC, Pang PS, Symonds WT, McHutchison JG, Muir AJ, Mangia A, Marcellin P (2014) *N Engl J Med* 370(20):1889–1898
45. Afdhal N, Reddy KR, Nelson DR, Lawitz E, Gordon SC, Schiff E, Nahass R, Ghalib R, Gitlin N, Herring R, Lalezari J, Younes ZH, Pockros PJ, di Bisceglie AM, Arora S, Subramanian GM, Zhu Y, Dvory-Sobol H, Yang JC, Pang PS, Symonds WT, McHutchison JG, Muir AJ, Sulkowski M, Kwo P (2014) *N Engl J Med* 370(16):1483–1493
46. Kowdley KV, Gordon SC, Reddy KR, Rossaro L, Bernstein DE, Lawitz E, Shiffman ML, Schiff E, Ghalib R, Ryan M, Rustgi V, Chojkier M, Herring R, Di Bisceglie AM, Pockros PJ, Subramanian GM, An D, Svarovskaia E, Hyland RH, Pang PS, Symonds WT, McHutchison JG, Muir AJ, Pound D, Fried MW (2014) *N Engl J Med* 370:1879–1888
47. Naggie S, Cooper C, Saag M, Workowski K, Ruane P, Towner WJ, Marks K, Luetkemeyer A, Baden RP, Sax PE, Gane E, Santana-Bagur J, Stamm LM, Yang JC, German P, Dvory-Sobol H, Ni L, Pang PS, McHutchison JG, Stedman CA, Morales-Ramirez JO, Bräu N, Jayaweera D, Colson AE, Tebas P, Wong DK, Dieterich D, Sulkowski M (2015) *N Engl J Med* 373:705–713
48. Feld JJ, Jacobson IM, Hezode C, Asselah T, Ruane PJ, Gruener N, Abergel A, Mangia A, Lai CL, Chan HL, Mazzotta F, Moreno C, Yoshida E, Shafraan SD, Towner WJ, Tran TT, McNally J, Osinusi A, Svarovskaia E, Zhu Y, Brainard DM, McHutchison JG, Agarwal K, Zeuzem S (2015) *N Engl J Med* 373:2599
49. Strader DB, Seeff LB (2012) *Clin Liver Dis* 1:6
50. Hoofnagle JH, Seeff LB (2006) *N Engl J Med* 355:2444
51. Backus LI, Belperio PS, Shahoumian TA, Loomis TP, Mole LA (2016) *Hepatology* 64:405–414
52. US Medicine. <http://www.usmedicine.com/agencies/department-of-veterans-affairs/va-could-soon-achieve-near-complete-eradication-of-hepatitis-c/>. Accessed 16 June 2018
53. Younossi ZM, Park H, Gordon SC, Ferguson JR, Ahmed A, Dieterich D, Saab S (2016) *Am J Manag Care* 22. (6 Spec No)
54. Eichler HG, Abadie E, Breckenridge A, Flamion B, Gustafsson LL, Leufkens H, Rowland M, Schneider CK, Bloechl-Daum B (2011) *Nat Rev Drug Discov* 10:495–506